

## Continuous Loading of Ultracold Ground-State $^{85}\text{Rb}_2$ Molecules in a Dipole Trap Using a Single Light Beam

Henry Fernandes Passagem,<sup>1</sup> Ricardo Colín-Rodríguez,<sup>1</sup> Jonathan Tallant,<sup>1</sup> Paulo Cesar Ventura da Silva,<sup>1</sup>

Nadia Bouloufa-Maafa,<sup>2</sup> Olivier Dulieu,<sup>2</sup> and Luis Gustavo Marcassa<sup>1,\*</sup>

<sup>1</sup>*Instituto de Física de São Carlos, Universidade de São Paulo, Caixa Postal 369, 13560-970, São Carlos, São Paulo, Brazil*

<sup>2</sup>*Laboratoire Aimé Cotton, CNRS, Université Paris-Sud, ENS Cachan, Université Paris-Saclay, 91405 Orsay cedex, France*



(Received 25 July 2018; revised manuscript received 10 February 2019; published 26 March 2019)

We have developed an approach to continuously load ultracold  $^{85}\text{Rb}_2$  vibrational ground-state molecules into a crossed optical dipole trap from a magneto-optical trap. The technique relies on a single high-power light beam with a broad spectrum superimposed onto a narrow peak at an energy of about  $9400\text{ cm}^{-1}$ . This single laser source performs all the required steps: the short-range photoassociation creating ground-state molecules after radiative emission, the cooling of the molecular vibrational population down to the lowest vibrational level  $v_X = 0$ , and the optical trapping of these molecules. Furthermore, we probe by depletion spectroscopy and determine that 75% of the  $v_X = 0$  ground-state molecules are in the three lowest rotational levels  $J_X = 0, 1, 2$ . The lifetime of the ultracold molecules in the optical dipole trap is limited to about 70 ms by off-resonant light scattering. The proposed technique opens perspectives for the formation of new molecular species in the ultracold domain, which are not yet accessible by well-established approaches.

DOI: [10.1103/PhysRevLett.122.123401](https://doi.org/10.1103/PhysRevLett.122.123401)

The development of cooling and trapping techniques for diatomic polar molecules is motivated by their wide range of potential applications, which are associated with their long-range dipole-dipole interaction and complex internal structure. Spectroscopy in cold trapped molecules has the potential to improve fundamental physics tests, such as parity violation [1,2], searches of fundamental constant variation [3,4], and measurement of the electron electric dipole moment [5–8]. A novel chemistry controlled at the single quantum-state level is also expected to play an important role in such cold samples [9,10]. Cold trapped polar molecules have also been proposed for quantum computation [11,12] as well as a simulator of strongly interacting quantum systems [11,13].

While such applications are all very exciting, the production of a cold and dense molecular sample is still very challenging. So, two classes of approaches have been developed over the last two decades. On one hand, various techniques employing cold buffer gas [14], electric [15–17], magnetic [18–20], and optical [21] external fields are directly applied to preformed molecules. Note that, until recently [22,23], laser cooling could not be applied directly to molecules because they generally do not possess suitable closed optical transitions, like in atomic systems. Only in the last few years have direct laser cooling and magneto-optical trapping of SrF [22] and CaF [23] been demonstrated. This technique remains limited to a small class of molecules that presents an almost closed transition, still necessitating, however, the generation of numerous laser

frequencies. On the other hand, a pair of ultracold atoms can be bonded either by photoassociation (PA) followed by radiative emission (RE) [24–26] or by magnetoassociation (MA) via a magnetic Feshbach resonance [27–31]. Both techniques face important limitations. The ground-state molecules created by PA and RE are spread over many vibrational levels with weak or moderate binding energies. Only a few PA schemes were able to produce  $v_X = 0$  molecules [32–38]. Those created by MA necessitate quantum degenerated ultracold atomic gases to adequately match the mediating Feshbach resonance and are formed in weakly bound levels that are collisionally unstable. An additional step of population transfer by optical means toward more stable levels is required. Therefore, the development of techniques that can be applied to any molecule is still an ongoing motivation.

In this Letter, we have developed a technique to continuously load  $^{85}\text{Rb}_2$  ground-state molecules into a crossed optical dipole trap from a standard magneto-optical trap (MOT) using a single light beam. The light beam is composed of a single-frequency coherent light source, which is responsible for short-range PA of cold rubidium atoms [39,40], and an incoherent broadband light source, which pumps the molecules created in various vibrational levels ( $v_X$ ) of the  $X^1\Sigma_g^+$  ground state, toward  $v_X = 0$ . This optical-pumping technique was first demonstrated in [41], but was never used to produce a sample of trapped molecules. We show that about 20 cycles of absorption and emission are necessary to optically pump 99% of the

molecular vibrational population into the  $v_X = 0$  level. We have also performed depletion spectroscopy of such molecules, revealing that about 75% of the  $v_X = 0$  molecules are in  $J = 0, 1, 2$  rotational states. Because of its high power, the same light beam is employed for trapping the molecules in a crossed optical dipole trap (ODT). Its lifetime is limited by off-resonant photon scattering.

The experiment setup and procedure have been described elsewhere [40]. The generation of a single light beam, for the ODT, is the key factor in our experiment. The high-power light beam is generated by a 50 W single-frequency fiber amplifier (IPG, model YAR-50K-1064-SF), which can operate in the 1060–1070 nm range [40]. Such an amplifier is seeded by a combination of a single-frequency grating-stabilized diode laser and a broadband superluminescent diode (SLD). The diode laser line width is below 1 MHz in the 1062–1070 nm range, and its frequency is locked to a commercial wave meter (HighFinesse, model WS-7). The broadband light is obtained using a SLD (QPhotonics, model QSDMI-1060-300), whose central wave number is around  $9430 \text{ cm}^{-1}$  and spectral bandwidth is about  $180 \text{ cm}^{-1}$ .

The processes induced by such a source are illustrated in Fig. 1. Two cold  $^{85}\text{Rb}$  atoms colliding in the  $X^1\Sigma_g^+$  electronic ground-state potential are photoassociated by the high-power light beam at  $9379.5 \text{ cm}^{-1}$  or  $1066.1 \text{ nm}$  (arrow 1), to the deeply bound rovibrational level  $v' = 138$ ,  $J' = 1$  (bound by  $3374.7 \text{ cm}^{-1}$  with respect to the  $5S + 5P_{1/2}$  dissociation limit) of the spin-orbit (SO)-coupled  $0_u^+(A^1\Sigma_u^+, b^3\Pi_u)$  excited electronic states [42]. Because of selection rules for dipole-allowed transitions in homonuclear dimers, the PA molecules decay by spontaneous emission (arrow 2) into a broad range of vibrational levels  $v_X$  of  $X^1\Sigma_g^+$  [39]. Note that this is in contrast to heteronuclear alkali molecules for which the decay can also occur down to the  $a^3\Sigma^+$  state. According to our modeling [39], the population of these molecules is distributed over levels  $10 < v_X < 120$  (purple vertical bar in Fig. 1), but mostly over ten vibrational levels ( $79 < v_X < 89$ ) bound by about  $500 \text{ cm}^{-1}$ .

The broadband spectrum of the source couples a wide set of transitions between  $v_X$  levels and  $0_u^+ v'$  levels (thick arrow 3 in Fig. 1). We shape its profile in order to exclude wave numbers larger than  $9539.4 \text{ cm}^{-1}$  corresponding to the ( $v_X = 1 \rightarrow v' = 0$ ) transition [42]. Thus the population of the  $v_X = 0$  is never repumped and it increases with time, while this level is not populated at all during a single PA-RE step via  $v' = 138$ . Figure 2 shows the resulting light spectrum before and after amplification, recorded using an optical spectrum analyzer (Anritsu, model MS9710C). Clearly, the amplifier gain curve plays a role in the final amplified spectrum: (i) the center of the broadband spectrum is shifted towards smaller energies, (ii) the output spectrum presents modulations that are associated with the amplifier itself [44], and (iii) the high-frequency cutoff has decreased.

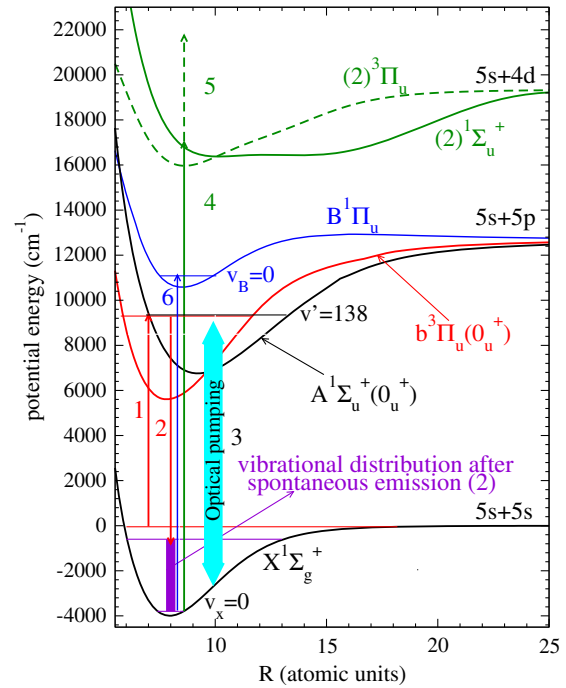


FIG. 1. Computed  $\text{Rb}_2$  Hund's case of potential energy curves [43] relevant for the present Letter. Processes induced by the light source are represented by arrows. (1) Short-range PA from the continuum of the  $X^1\Sigma_g^+$  ground state toward the rovibrational level  $v' = 138$ ,  $J' = 1$  (bound by  $3374.7 \text{ cm}^{-1}$  with respect to the  $5S + 5P_{1/2}$  dissociation limit) of the spin-orbit (SO)-coupled  $0_u^+(A^1\Sigma_u^+, b^3\Pi_u)$ -coupled states, achieved by the peak part of the laser spectrum at  $9379.5 \text{ cm}^{-1}$ . (2) Spontaneous emission back to  $X^1\Sigma_g^+$  levels, thus creating ultracold molecules in a distribution of levels represented by the purple vertical bar. (3) Optical pumping of the vibrational distribution of the ultracold molecules induced by the broadband part of the light source. (4), (5) RE2PI detection of  $\text{Rb}_2^+$  ions. (6) Rotational-state depletion spectroscopy of  $v_X = 0, J_X$  molecules.

The ground-state molecules are detected by a resonantly enhanced 2-photon ionization (RE2PI) via the  $(2)^1\Sigma_u^+$  excited state (arrows 4 and 5 in Fig. 1). The ionization step is achieved by a pulsed dye laser (Jaguar, Continuum, 1 mJ per pulse, 5 ns duration, and 20 Hz repetition rate) pumped by the third harmonic of a pulsed Nd:YAG laser, operating at wave numbers ranging between  $20855$  and  $20985 \text{ cm}^{-1}$ . The pulsed dye laser is focused to a width of  $250 \pm 50 \mu\text{m}$  at the position of the crossed ODT. The  $\text{Rb}_2^+$  ions are detected by an ion counter [40].

Figure 3(a) shows the experimental  $\text{Rb}_2^+$  spectrum in the absence of the broadband light source; i.e., only the PA diode laser beam is injected into the fiber amplifier. The ions are counted for 200 dye laser pulses and each spectrum is an average of ten measurements. Starting from our previous work [40], we have modeled the transitions [with Franck-Condon factors (FCFs) larger than  $10^{-3}$ ] that can be accessed by the pulsed dye laser from the  $v_X$  levels populated after a single PA-RE cycle through the  $v' = 138, J' = 1$  level to the  $(2)^1\Sigma_u^+$  levels. The experimental

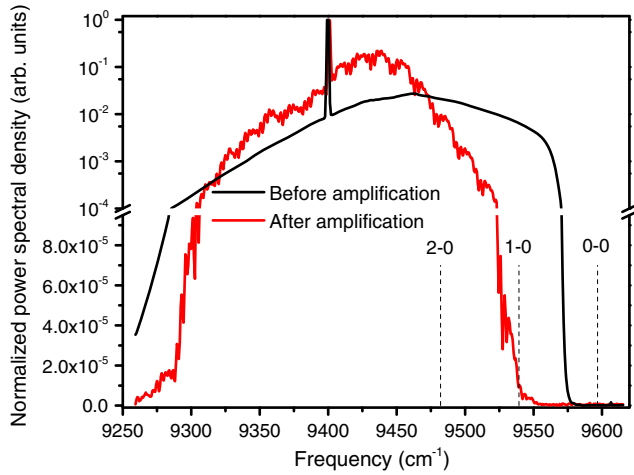


FIG. 2. Laser and SLD combined light spectrum before and after amplification. Note the break in the vertical scale. The vertical lines represent transition energies from the  $v_X = 0, 1, 2$  levels of  $X^1\Sigma_g^+$  to  $v' = 0$  of the  $0_u^+$ -coupled states. The 0-0 transition is indeed excluded from the amplified light spectrum.

spectrum exhibits more peaks than the simulated one, complicating the assignment of the peaks. Several reasons for this discrepancy are possible: (i) the inaccuracy of the energy position of the  $(2)^1\Sigma_u^+$  vibrational levels (also

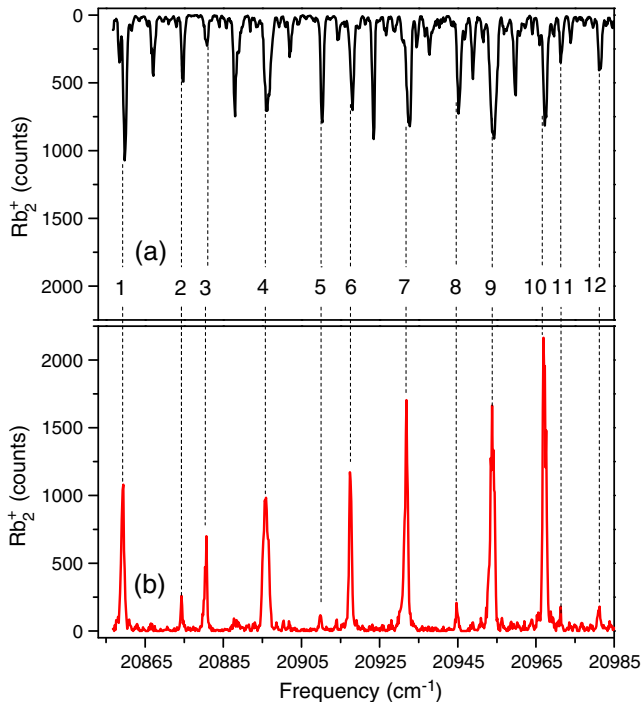


FIG. 3. RE2PI spectra recorded when the PA laser frequency is locked at  $9379.5 \text{ cm}^{-1}$ . The spectra are associated with excitation of  $X^1\Sigma_g^+$  levels towards coupled  $(2)^1\Sigma_u^+ - (2)^3\Pi_u$  levels, which are then ionized. (a) Without and (b) with optical pumping induced by the broadband part of the light spectrum. (b) The peaks are numbered from 1 to 12, and their correspondence with those in (a) is highlighted with dashed lines.

quoted in Ref. [45]), based on our computed  $(2)^1\Sigma_u^+$  potential curve; (ii) the SO coupling between the  $(2)^1\Sigma_u^+$  and the  $(2)^3\Pi_u$  excited states, arbitrarily fixed in our model by the (small) Rb( $4d$ ) SO splitting ( $0.46 \text{ cm}^{-1}$ ), in the absence of any other data; it is most probably underestimated in the molecular region, thus reducing the number of accessible levels. But more importantly, we show in the Supplemental Material that the high-power PA laser ( $\sim 4 \text{ MW cm}^{-2}$ ) [46], which operates continuously, can also perform vibrational cooling even when the broadband component is absent, strongly modifying the  $v_X$  population compared to a single PA-RE step. In particular, the model reveals that the  $v_X = 0$  can be populated after 17 PA-RE cycles (see Fig. S5 of the Supplemental Material).

When the broadband spectrum is seeded into the fiber amplifier [Fig. 3(b)], the number of peaks is drastically reduced to 12 well-resolved peaks in the displayed range ( $20853\text{--}20985 \text{ cm}^{-1}$ ), half of them with an amplitude larger than in Fig. 3(a). The positions of these peaks are reported in the Supplemental Material [46]. Following Fig. 2, we expect that most of these peaks should be associated with the ionization of  $v_X = 0$  molecules. We note that several of these peaks were already present in Fig. 3(a), which would support the model for the vibrational pumping induced by the PA laser alone. It is striking that a pattern in energy and intensity seems to be replicated among the triplets of lines (2–4), (5–7), and (8–10). We are currently working at assigning these peaks, relying in particular on the data of Ref. [45], and this will be the purpose of another study.

In addition, we have performed the depletion spectroscopy [49] of these lines to probe that the formed molecules are in the  $v_X = 0$  level. We have used a diode laser at  $682 \text{ nm}$  (with an intensity of  $\sim 200 \text{ mW cm}^{-2}$ ) to drive transitions from  $v_X = 0, J_X$  to  $v_B = 0, J_B$  of the  $B^1\Pi_u$  potential (arrow 6 in Fig. 1). Figure 4 shows a depletion spectrum performed on peak 10 and similar ones recorded for the most intense peaks 9, 7, 6, 4, 3, 1. The remaining peaks are too weak for this spectroscopy. The depletion is indeed efficient, probing that these series of peaks originates from  $v_X = 0$ . As expected, the rotational structure of the lines is resolved, and their intensities allow us to determine that 75% of the  $v_X = 0$  molecules lie in  $J_X = 0, 1, 2$  rotational levels, which implies that the remaining ones should be in higher rotational levels. The present experiment is similar to the  $\text{Cs}_2$  experiment [41]; therefore it is not surprising that the rotational population distribution in  $\text{Rb}_2$  is similar to the  $\text{Cs}_2$  results [50]. Our simulations show (see the Supplemental Material [46]) that, after the PA molecules have gone through their first spontaneous decay, they require about 20 cycles of absorption and emission with the amplified broadband source to be pumped into  $v_X = 0$  with an efficiency of 99%, while only 1% of the initial distribution remains in  $v_X > 0$ , which we estimate [according to spectra in Figs. 3(a) and 3(b)] to be about 5%.

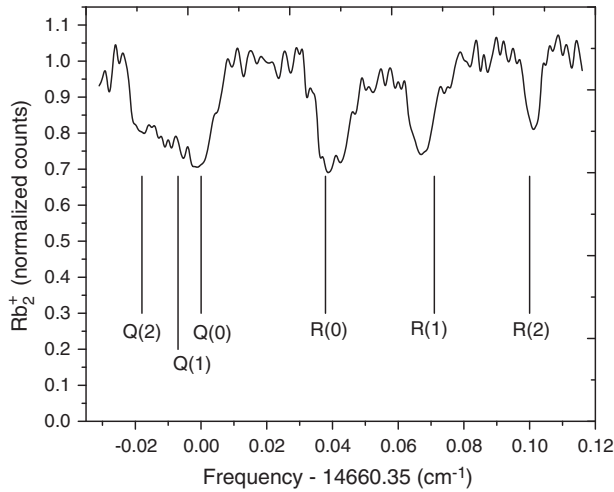


FIG. 4. Depletion spectrum of peak 10 (at  $20966.9 \text{ cm}^{-1}$ ) in Fig. 3(b), when the depletion laser is tuned at the energy of the transition ( $v_X = 0, J_X \rightarrow v_B = 0, J_B$ ). The origin of the spectrum is set at the energy of the ( $v_X = 0, J_X = 0 \rightarrow v_B = 0, J_B = 0$ )  $Q(0)$  transition at  $14660.35 \text{ cm}^{-1}$ . The vertical bars show the expected position of the lines, using the spectroscopic data of Ref. [51]. They are labeled with conventional spectroscopic notation, i.e.,  $Q(J_X)$  for ( $v_X = 0, J_X \rightarrow v_B = 0, J_X$ ) and  $R(J_X)$  for ( $v_X = 0, J_X \rightarrow v_B = 0, J_X + 1$ ).

Such ultracold ground-state molecules are trapped by the same light beam responsible for their formation. To demonstrate this, we first switched on the MOT and ODT lasers, recalling that the molecules are loaded from a standard MOT. We measured the molecular population as a function of time during 1 s. After 1 s, we turned off the MOT and observed the molecular population decay time. The PA diode laser frequency was tuned to  $9379.5 \text{ cm}^{-1}$  and the RE2PI laser to  $20966.9 \text{ cm}^{-1}$ . This ionization energy corresponds to peak 10 in Fig. 3(b), to ensure the best signal-to-noise ion ratio. Figure 5 shows the time evolution of the molecule population. Each experimental point results from an average over 500 RE2PI laser pulses. By fitting the experimental curve, we can obtain a characteristic loading time of  $66 \pm 3 \text{ ms}$  (data below 1 s) and a decay time of  $80 \pm 2 \text{ ms}$  in the ODT (data above 1 s), which are mainly due to off-resonant transitions between  $v_X = 0$  and the  $0_u^+ v' = 0$  level (see Supplemental Material [46]). The molecular ODT holds about  $10^4$  molecules in  $v_X = 0$ , at an estimated density of  $10^{10} \text{ cm}^{-3}$  [52].

In this Letter, we have developed a novel approach to continuously produce and trap ultracold  $^{85}\text{Rb}_2$  ground-state molecules in the lowest vibrational level  $v_X = 0$  starting from a standard magneto-optical trap. In contrast to previous works reported in the literature, this technique relies on the use of a single high-power light beam that performs all the required functions: photoassociation, internal vibrational cooling, and optical trapping of the molecules. We have demonstrated that  $\sim 10^4$  molecules can

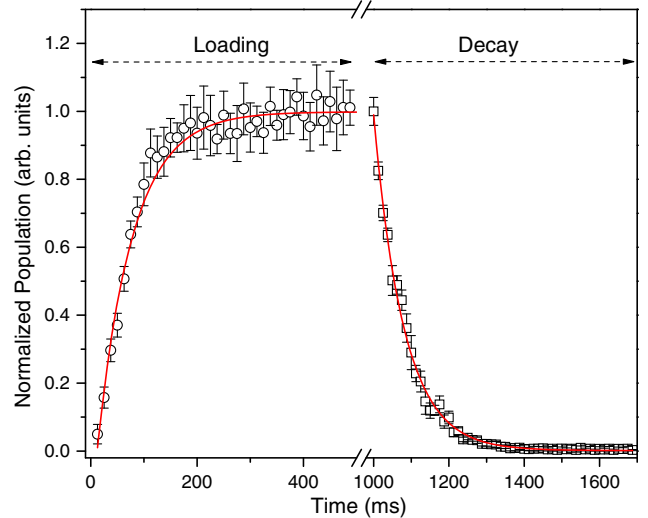


FIG. 5. Evolution of the vibrational ground-state molecule population as a function of time during the loading (below 1 s, MOT on) stage, and when the MOT is switched off (above 1 s), thus reflecting the loss from the ODT. The red lines are exponential fits.

be trapped in an optical dipole trap at a density of about  $10^{10} \text{ cm}^{-3}$ . The ODT lifetime is limited due to off-resonant photon scattering, but this system could be used to investigate interactions between a ground-state molecule and a Rydberg atom [53]. This problem is mitigated by turning off the 1064 nm ODT and turning on an ODT at 1550 nm, which would result in a lifetime as long as 40 s according to our scattering model. The proposed technique could be applied to a variety of molecules that are not as convenient as alkali-metal dimers for ultracold molecule formation using magnetoassociation and adiabatic population transfer. One example is the quest for the formation of RbSr open-shell species [54,55], which possess both a magnetic moment and an intrinsic permanent electric dipole moment in its  $X^2\Sigma^+$  electronic ground state. If one uses an amplified light beam in the 1050–1080 nm range, which is commercially available, it would be possible to photoassociate RbSr molecules through the excited  $(2)^2\Sigma^+$  excited electronic state and pump them optically down to the  $v_X = 0$ . The FCFs for the optical pumping are favorable since both potentials have their minima around 8.7 bohr radii.

This work is supported by Grants No. 2011/23533-9, No. 2013/02816-8, and No. 2014/24479-6, São Paulo Research Foundation (FAPESP) and CNPq. This study was financed in part by the Coordenação de Aperfeiçoamento de Pessoal de Nível Superior—Brasil (CAPES)—Finance Code 001. We also acknowledge Cristian Adan Mojica Casique and Manuel Alejandro Lefran Torres for technical help in the depletion spectroscopy measurement.

\*marcassa@ifsc.usp.br

- [1] B. Darquié, C. Stoeffler, A. Shelkownikov, C. Daussy, A. AmyKlein, C. Chardonnet, S. Zrig, L. Guy, J. Crassous, P. Soulard, P. Asselin, T. R. Huet, P. Schwerdtfeger, R. Bast, and T. Saue, *Chirality* **22**, 870 (2010).
- [2] D. DeMille, S. B. Cahn, D. Murphree, D. A. Rahmlow, and M. G. Kozlov, *Phys. Rev. Lett.* **100**, 023003 (2008).
- [3] S. Truppe, R. Hendricks, S. Tokunaga, H. Lewandowski, M. Kozlov, H. Christian, E. Hinds, and M. Tarbutt, *Nat. Commun.* **4**, 2600 (2013).
- [4] E. R. Hudson, H. J. Lewandowski, B. C. Sawyer, and J. Ye, *Phys. Rev. Lett.* **96**, 143004 (2006).
- [5] S. Eckel, P. Hamilton, E. Kirilov, H. W. Smith, and D. DeMille, *Phys. Rev. A* **87**, 052130 (2013).
- [6] J. J. Hudson, D. M. Kara, I. J. Smallman, B. E. Sauer, M. R. Tarbutt, and E. A. Hinds, *Nature (London)* **473**, 493 (2011).
- [7] A. C. Vutha, W. C. Campbell, Y. V. Gurevich, N. R. Hutzler, M. Parsons, D. Patterson, E. Petrik, B. Spaun, J. M. Doyle, G. Gabrielse, and D. DeMille, *J. Phys. B* **43**, 074007 (2010).
- [8] J. Baron, W. C. Campbell, D. DeMille, J. M. Doyle, G. Gabrielse, Y. V. Gurevich, P. W. Hess, N. R. Hutzler, E. Kirilov, I. Kozyryev, B. R. O'Leary, C. D. Panda, M. F. Parsons, E. S. Petrik, B. Spaun, A. C. Vutha, and A. D. West, *Science* **343**, 269 (2014).
- [9] R. V. Krems, *Phys. Chem. Chem. Phys.* **10**, 4079 (2008).
- [10] N. Balakrishnan and A. Dalgarno, *Chem. Phys. Lett.* **341**, 652 (2001).
- [11] A. André, D. DeMille, J. M. Doyle, M. D. Lukin, S. E. Maxwell, P. Rabl, R. J. Schoelkopf, and P. Zoller, *Nat. Phys.* **2**, 636 (2006).
- [12] D. DeMille, *Phys. Rev. Lett.* **88**, 067901 (2002).
- [13] A. Micheli, G. K. Brennen, and P. Zoller, *Nat. Phys.* **2**, 341 (2006).
- [14] J. D. Weinstein, R. de Carvalho, T. Guillet, B. Friedrich, and J. M. Doyle, *Nature (London)* **395**, 148 (1998).
- [15] H. L. Bethlem, G. Berden, and G. Meijer, *Phys. Rev. Lett.* **83**, 1558 (1999).
- [16] H. L. Bethlem, G. Berden, F. M. H. Crompvoets, R. T. Jongma, A. J. A. van Rooij, and G. Meijer, *Nature (London)* **406**, 491 (2000).
- [17] J. van Veldhoven, H. L. Bethlem, and G. Meijer, *Phys. Rev. Lett.* **94**, 083001 (2005).
- [18] B. C. Sawyer, B. L. Lev, E. R. Hudson, B. K. Stuhl, M. Lara, J. L. Bohn, and J. Ye, *Phys. Rev. Lett.* **98**, 253002 (2007).
- [19] N. Vanhaecke, U. Meier, M. Andrist, B. H. Meier, and F. Merkt, *Phys. Rev. A* **75**, 031402 (2007).
- [20] E. Narevicius, A. Libson, C. G. Parthey, I. Chavez, J. Narevicius, U. Even, and M. G. Raizen, *Phys. Rev. A* **77**, 051401 (2008).
- [21] R. Fulton, A. I. Bishop, and M. N. Shneider, and P. F. Barker, *Nat. Phys.* **2**, 465 (2006).
- [22] J. F. Barry, D. J. McCarron, E. B. Norrgard, M. H. Steinecker, and D. DeMille, *Nature (London)* **512**, 286 (2014).
- [23] S. Truppe, H. J. Williams, L. Hambach, M. Caldwell, N. J. Fitch, E. A. Hinds, B. E. Sauer, and M. R. Tarbutt, *Nat. Phys.* **13**, 1173 (2017).
- [24] H. R. Thorsheim, J. Weiner, and P. S. Julienne, *Phys. Rev. Lett.* **58**, 2420 (1987).
- [25] K. M. Jones, E. Tiesinga, P. D. Lett, and P. S. Julienne, *Rev. Mod. Phys.* **78**, 483 (2006).
- [26] A. Fioretti, D. Comparat, A. Crubellier, O. Dulieu, F. Masnou-Seeuws, and P. Pillet, *Phys. Rev. Lett.* **80**, 4402 (1998).
- [27] S. Ospelkaus, K.-K. Ni, D. Wang, M. H. G. de Miranda, B. Neyenhuis, G. Quéméner, P. S. Julienne, J. L. Bohn, D. S. Jin, and J. Ye, *Science* **327**, 853 (2010).
- [28] T. Takekoshi, L. Reichsöllner, A. Schindewolf, J. M. Hutson, C. R. Le Sueur, O. Dulieu, F. Ferlaino, R. Grimm, and H.-C. Nägerl, *Phys. Rev. Lett.* **113**, 205301 (2014).
- [29] P. K. Molony, P. D. Gregory, Z. Ji, B. Lu, M. P. Köppinger, C. R. Le Sueur, C. L. Blackley, J. M. Hutson, and S. L. Cornish, *Phys. Rev. Lett.* **113**, 255301 (2014).
- [30] J. W. Park, S. A. Will, and M. W. Zwiernlein, *Phys. Rev. Lett.* **114**, 205302 (2015).
- [31] M. Guo, B. Zhu, B. Lu, X. Ye, F. Wang, R. Vexiau, N. Bouloufa-Maafa, G. Quéméner, O. Dulieu, and D. Wang, *Phys. Rev. Lett.* **116**, 205303 (2016).
- [32] J. Deiglmayr, A. Grochola, M. Repp, K. Mörtlbauer, C. Glück, J. Lange, O. Dulieu, R. Wester, and M. Weidemüller, *Phys. Rev. Lett.* **101**, 133004 (2008).
- [33] P. Zabawa, A. Wakim, M. Haruza, and N. P. Bigelow, *Phys. Rev. A* **84**, 061401 (2011).
- [34] C. Gabbanini and O. Dulieu, *Phys. Chem. Chem. Phys.* **13**, 18905 (2011).
- [35] J. Banerjee, D. Rahmlow, R. Carollo, M. Bellos, E. E. Eyler, P. L. Gould, and W. C. Stwalley, *Phys. Rev. A* **86**, 053428 (2012).
- [36] C. D. Bruzewicz, M. Gustavsson, T. Shimasaki, and D. DeMille, *New J. Phys.* **16**, 023018 (2014).
- [37] I. C. Stevenson, D. B. Blasing, Y. P. Chen, and D. S. Elliott, *Phys. Rev. A* **94**, 062510 (2016).
- [38] Z. Li, T. Gong, Z. Ji, Y. Zhao, L. Xiao, and S. Jia, *Phys. Chem. Chem. Phys.* **20**, 4893 (2018).
- [39] C. R. Menegatti, B. S. Marangoni, N. Bouloufa-Maafa, O. Dulieu, and L. G. Marcassa, *Phys. Rev. A* **87**, 053404 (2013).
- [40] H. F. Passagem, R. Colin-Rodriguez, P. C. V. da Silva, N. Bouloufa-Maafa, O. Dulieu, and L. G. Marcassa, *J. Phys. B* **50**, 045202 (2017).
- [41] M. Viteau, A. Chotia, M. Allegrini, N. Bouloufa, O. Dulieu, D. Comparat, and P. Pillet, *Science* **321**, 232 (2008).
- [42] T. Bergeman, J. Qi, D. Wang, Y. Huang, H. K. Pechkis, E. E. Eyler, P. L. Gould, W. C. Stwalley, R. A. Cline, J. D. Miller, and D. J. Heinzen, *J. Phys. B* **39**, S813 (2006).
- [43] J. Lozeille, A. Fioretti, C. Gabbanini, Y. Huang, H. K. Pechkis, D. Wang, P. L. Gould, E. E. Eyler, W. C. Stwalley, M. Aymar, and O. Dulieu, *Eur. Phys. J. D* **39**, 261 (2006).
- [44] IPG Photonics Collaboration (private communication).
- [45] Y. Huang, J. Qi, H. K. Pechkis, D. Wang, E. E. Eyler, P. L. Gould, and W. C. Stwalley, *J. Phys. B* **39**, S857 (2006).
- [46] See Supplemental Material at <http://link.aps.org/supplemental/10.1103/PhysRevLett.122.123401> for detailed explanation of vibrational cooling by the high-power laser, which includes Refs. [47,48].
- [47] M. Deiß, B. Drews, J. H. Denschlag, N. Bouloufa-Maafa, R. Vexiau, and O. Dulieu, *New J. Phys.* **17**, 065019 (2015).
- [48] V. Kokouline, O. Dulieu, R. Kosloff, and F. Masnou-Seeuws, *J. Chem. Phys.* **110**, 9865 (1999).
- [49] D. Wang, J. T. Kim, C. Ashbaugh, E. E. Eyler, P. L. Gould, and W. C. Stwalley, *Phys. Rev. A* **75**, 032511 (2007).

- [50] I. Manai, R. Horchani, H. Lignier, P. Pillet, D. Comparat, A. Fioretti, and M. Allegrini, *Phys. Rev. Lett.* **109**, 183001 (2012).
- [51] C. Amiot and J. Vergès, *Chem. Phys. Lett.* **274**, 91 (1997).
- [52] A. R. L. Caires, V. A. Nascimento, D. C. J. Rezende, V. S. Bagnato, and L. G. Marcassa, *Phys. Rev. A* **71**, 043403 (2005).
- [53] J. A. Fernández, P. Schmelcher, and R. González-Férez, *J. Phys. B* **49**, 124002 (2016).
- [54] P. S. Żuchowski, R. Guérout, and O. Dulieu, *Phys. Rev. A* **90**, 012507 (2014).
- [55] A. Ciamei, J. Szczepkowski, A. Bayerle, V. Barbé, L. Reichsöllner, S. M. Tzanova, C.-C. Chen, B. Pasquiou, A. Grochola, P. Kowalczyk, W. Jastrzebski, and F. Schreck, *Phys. Chem. Chem. Phys.* **20**, 26221 (2018).